

## Monolithic Polycapillary Neutron Focusing Lenses: Experimental Characterizations

H. H. Chen-Mayer, D. F. R. Mildner,

\*V. A. Sharov, \*J. B. Ullrich, \*I. Yu. Ponomarev, \*and R. G. Downing

*Chemical Science and Technology Laboratory, National Institute of Standards and Technology, Gaithersburg,  
MD 20899, USA*

*\*X-Ray Optical Systems, Inc., Albany, NY 12205, USA*

(Received 15 March 1996; accepted 15 May 1996)

Multifiber polycapillary optics have been used for guiding and focusing neutron beams based on the principle of total external reflection. A recent development involving the miniaturization of such neutron focusing lenses has produced monolithic bundles of tapered capillaries with higher fractional open area and smaller focal spot size compared to the previous generations of devices containing many polycapillary fibers. This paper presents experimental characterizations of two monolithic lenses using a cold neutron beam from a research reactor.

**KEYWORDS:** neutron focusing, neutron lens, neutron depth profiling, polycapillary optics

### 1. Introduction

Multifiber polycapillary optics<sup>1)</sup> have been used for guiding and focusing reactor-generated neutron beams to produce a small focus for material analysis<sup>2)</sup>. These lenses consist of thousands of polycapillary fibers; each fiber has parallel channels throughout the entire length. All fibers are curved and follow a designed pattern to create an intense focused beam on a sub-mm spot. Such lenses can accept an incident beam with a large cross section, and have achieved a current density gain of two orders of magnitude. However, because the fibers contain constant diameter channels, the concentration of the guided neutron beams must be achieved by bending the fibers following the various designed curvatures. Thus, these lenses have a significant percentage of the space not occupied by fibers at the entrance. As a result, the spatial capture efficiency of the lens is low. For example, a neutron lens<sup>3)</sup> for Prompt Gamma Activation Analysis at NIST utilizes only a few percent of the total incident beam from the exit of a <sup>58</sup>Ni-coated guide and a Be filtered white beam (average  $\lambda \sim 6\text{\AA}$ ). Despite the low efficiency, the gain in neutron current density on a 0.53 mm diameter (FWHM) spot is 80. As the spatial capture efficiency is improved, the gain will be pushed even higher. To address this issue, research has been underway at X-Ray Optical Systems, Inc<sup>4)</sup> to fabricate a newer generation of lenses which are monolithic. We report preliminary studies on prototypes of new lenses examined with a cold neutron beam.

### 2. Experimental Conditions

The measurements have been performed at the 30 MW High Flux Beam Reactor (HFBR) beam line H9C at Brookhaven National Laboratory. H9C is a natural Ni-coated neutron guide with a LN<sub>2</sub> cooled Be filter viewing the liquid hydrogen cold source. No monochromator is installed before the apparatus, and therefore a white beam with an estimated short-wavelength cut-off at about 4  $\text{\AA}$  (as measured with a mini-chopper<sup>5)</sup>) is used. The beam size is 43mm (V)  $\times$  15mm (H), and the current density is approximately  $1 \times 10^8$  n/cm<sup>2</sup>-s (thermal equivalent),

determined by gold foil activation analysis, at the sample position. The incident beam divergence is determined by measuring the beam spread after a 0.5 mm slit placed either vertically or horizontally. By measuring the FWHM of the beam size behind the slit at two distances, the full divergence is calculated to be about 18.6 mrad in both directions.

### 3. Monolithic Lens

A monolithic lens is a device made with a single piece of glass containing from thousands to millions of small channels that are parallel at the entrance and tapered toward a common axis at the exit, creating a focus at, for example, 20 mm from the exit. The lenses under study have a cross section that is hexagonal in shape, and the flat-to-flat distance is 4 and 2.5 mm at the entrance and exit, respectively. The fractional open area is estimated to be 50%. The lenses are designed and fabricated by X-Ray Optical Systems, Inc. In this experiment, two lenses have been tested (denoted as lens #1 and #2).

### 4. Transmission Measurements

The lens is placed in the neutron beam path, and aligned by rocking in the horizontal and vertical planes such that the transmitted intensity is maximized. The images of the transmitted beam along the beam path are recorded to determine the focal distance. The image is captured on an imaging detector (VRD—Video Radiation Detector<sup>6)</sup>), from which the current density gain can be determined by taking the ratio of the neutron beam intensity at the focal position with and without the lens. Figure 1 shows the image of the focused beam and the intensity distribution.

### 5. Data Analysis and Results

Each neutron beam image collected using the VRD (pixel size of  $12.5 \times 13.7 \mu\text{m}^2$ ) is stored in a file for off-line analysis.

First, a line (width of four pixels) profile is drawn across the image to obtain the intensity distribution. Such a profile is repeated in four orientations and an average is

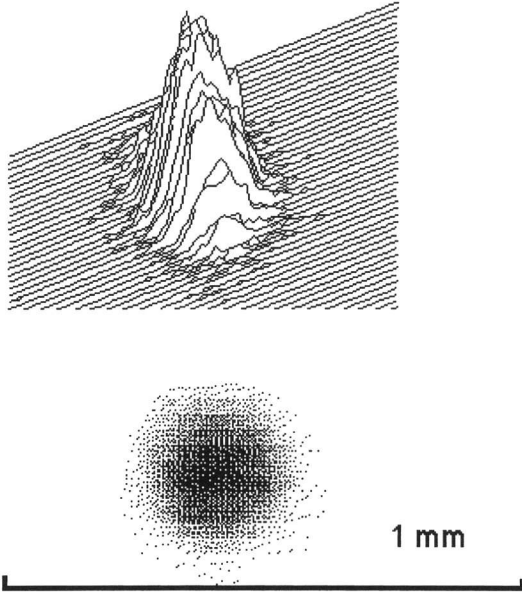


Fig. 1. Image of the focused beam (lower panel) captured by the VRD, and the spatial distribution of the intensity (upper panel).

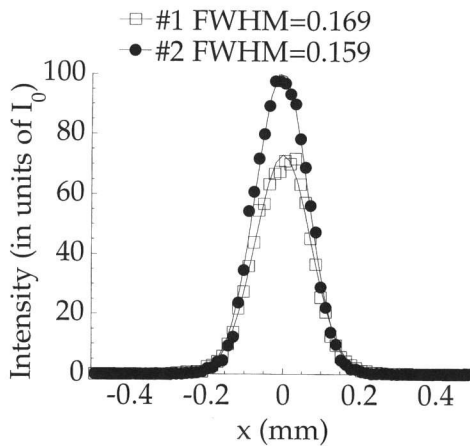


Fig. 2. Spatial distribution of intensity (normalized to that of the incident beam) at the focus for the two lenses (points) and their respective Gaussian fits (lines).  $I_0$  is the incident beam intensity.

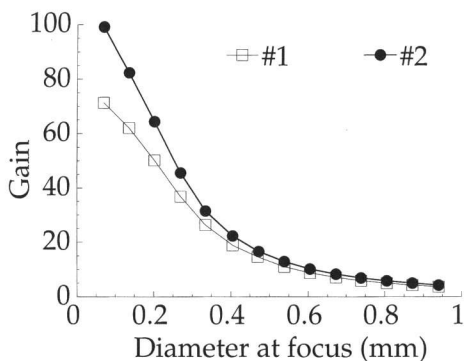


Fig. 3. The gain in current density as a function of diameter of the integrated area at the focus.

taken for better statistics. The resultant intensity distribution is then fitted to a Gaussian curve,

$$y = y_0 + y_m \exp\left[-(x - x_0)^2 / (2\sigma^2)\right],$$

where  $y_0$  represents the background level, and  $y_m$  the peak height, to determine the FWHM of the spot size. The intensity distribution at the focus for the two lenses and their respective Gaussian fits are shown in Figure 2. The FWHM thus determined are 0.169 mm and 0.159 mm for lenses #1 and #2, respectively.

Because of the Gaussian-like intensity distribution, the transmitted neutron beam intensity, and therefore the current density gain, depends on the sampling area. By integrating up to a certain radius, the total number of neutrons within this area can be determined. This value is then normalized to the incident beam, measured by removing the lens, to obtain the gain in current density. Figure 3 shows the gain as a function of diameter of the integrated area at the focus for both lenses. The results of two lenses are also summarized in Table 1.

The FWHM and the peak intensity are also determined for all images along the beam path, as shown in Figure 4, depicting the focusing and defocusing process.

## 6. Comparison with a multifiber lens

The monolithic lens is far more efficient in utilizing incident neutrons compared with a multifiber lens. However, the entrance area of the monolithic lens is much smaller (by a factor of  $\sim 160$ ) and therefore it captures a smaller absolute number of neutrons. Consequently, the total number of neutrons delivered to the focus is about 10 times higher for a multifiber lens. On the other hand, the focal area for the monolithic lens is more than 10 times

Table 1. Results of measurement at the focus

lens#	length of lens (mm)	focal length (mm)	focus FWHM (mm)	current density gain over FWHM
1	45	23	0.169	56
2	46.5	21	0.159	74

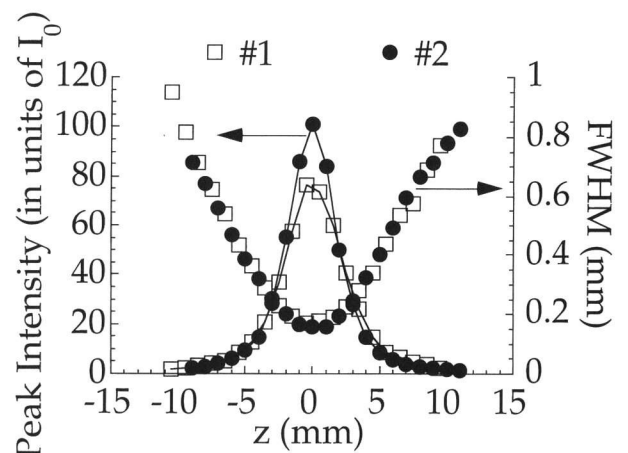


Fig. 4. FWHM and peak intensity (normalized to that of the incident beam) along the beam path.  $I_0$  is the incident beam intensity.

smaller than for the multifiber lens. These compensating factors result in a comparable gain in current density achieved for the monolithic and multifiber lens. The characteristics representative of the two types of lenses are listed in Table 2. A monolithic lens may be more suitable for applications entailing constrained space such as inside of a vacuum chamber, and for those involving small size (<0.5 mm) samples or small regions of interest of a large sample, such as in compositional mapping which desires a better spatial resolution. For example, Neutron Depth Profiling which employs the detection of charged particles emitted as a result of neutron absorption can benefit from using such a monolithic lens to increase the incident beam to the sample, and to define the probed region more precisely.

### Acknowledgment

We greatly appreciate the assistance from and helpful discussions with Larry Passell and staff at HFBR during the course of experiment. We also thank Richard Lindstrom of NIST for the gold foil activation measurement of the neutron beam current density. X-Ray Optical Systems acknowledges the partial support for this work by the Advanced Technology Program of NIST, agreement #70NANB2H1250, and by U. S. Department of Energy, grant #DE-FG02-92ER81411.

Table 2. Comparisons of characteristics of a multifiber lens<sup>3)</sup> and a monolithic lens, where

- $r_{\theta}$ : ratio of the critical angle of the lens material to the incident beam divergence;  
 $f$ : fractional open area of lens;  
 $I_{in}$ : fraction of neutrons incident on entrance face of lens which is captured by lens;  
 $r_A$ : ratio of entrance area to that of focal spot, and an area of  $2\pi\sigma^2$  of focal spot is assumed;  
 gain: measured gain in current density over FWHM ( $=2.35\sigma$ );  
 $I_{out}(= \text{gain}/ r_A)$ : fraction of neutrons incident on entrance face of lens which arrives at the focus.

lens	$r_{\theta}^2$	$f$	$I_{in}$	$r_a$	gain	$I_{out}$
multifiber	0.29	0.088	0.025	7031	80	0.011
monolithic	0.40	0.50	0.20	481	74	0.15

- 1) M. A. Kumakhov and V. A. Sharov, *Nature* 357, 390, (1992)  
 H. Chen, R. G. Downing, D. F. R. Mildner, W. M. Gibson, M. A. Kumakhov, I. Yu. Ponomarev, and M. V. Gubarev, *Nature* 357, 391 (1992)  
 2) H. Chen, V. A. Sharov, D. F. R. Mildner, R. G. Downing, R. L. Paul, R. M. Lindstrom, C. J. Zeissler, and Q. F. Xiao, *Nucl. Inst. Meth. B* 95, 107 (1995)  
 3) Q. F. Xiao, H. Chen, V. A. Sharov, D. F. R. Mildner, R. G. Downing, N. Gao, and D. M. Gibson, *Rev. Sci. Inst.*, 65, 3399 (1994)  
 4) N. Gao, I. Yu. Ponomarev, Q. F. Xiao, W. M. Gibson, and D. A. Carpenter, to be published  
 Q. F. Xiao and N. Gao, *29th Annual Microbeam Analysis Society Meeting*, Breckenridge, CO, August 6-11, 1995  
 5) R. E. Benenson, V. A. Sharov, and H. H. Chen-Mayer, *Rev. Sci. Inst.*, to be published  
 6) R. G. Downing, C. J. Zeissler, and H. Chen, *SPIE Conference Proceedings* 1737, 308 (1993)